MOLECULAR AND CELLULAR BIOLOGY, Aug. 1993, p. 4691–4702
0270-7306/93/084691-12$02.00/0
Copyright © 1993, American Society for Microbiology
Vol. 13, No. 8

CSE1 and *CSE2*, Two New Genes Required for Accurate Mitotic Chromosome Segregation in *Saccharomyces cerevisiae*

ZHIXIONG XIAO,† JEFFERY T. McGREW,‡ ANDREW J. SCHROEDER, AND MOLLY FITZGERALD-HAYES*

Department of Biochemistry and Molecular Biology, Program in Molecular and Cellular Biology, University of Massachusetts, Amherst, Massachusetts 01003

Received 15 January 1993/Returned for modification 19 February 1993/Accepted 6 May 1993

By monitoring the mitotic transmission of a marked chromosome bearing a defective centromere, we have identified conditional alleles of two genes involved in chromosome segregation (*cse*). Mutations in *CSE1* and *CSE2* have a greater effect on the segregation of chromosomes carrying mutant centromeres than on the segregation of chromosomes with wild-type centromeres. In addition, the *cse* mutations cause predominantly nondisjunction rather than loss events but do not cause a detectable increase in mitotic recombination. At the restrictive temperature, *cse1* and *cse2* mutants accumulate large-budded cells, with a significant fraction exhibiting aberrant binucleate morphologies. We cloned the *CSE1* and *CSE2* genes by complementation of the cold-sensitive phenotypes. Physical and genetic mapping data indicate that *CSE1* is linked to *HAP2* on the left arm of chromosome VII and *CSE2* is adjacent to *PRP2* on chromosome XIV. *CSE1* is essential and encodes a novel 109-kDa protein. *CSE2* encodes a 17-kDa protein with a putative basic-region leucine zipper motif. Disruption of *CSE2* causes chromosome missegregation, conditional lethality, and slow growth at the permissive temperature.

During cell division, the transmission of each chromosome depends on many complex mechanisms. Although the molecular details involved in these processes are not yet clear for any system, the relative structural simplicity and convenient genetic assays for the budding yeast *Saccharomyces cerevisiae* make this organism an excellent system for the study of chromosome segregation. In addition, the centromere DNA has been cloned from yeast chromosomes and extensively analyzed. A completely functional *S. cerevisiae* centromere consists of about 120 bp containing three conserved DNA elements (CDE); an extremely AT-rich central element, CDEII, is flanked by CDEI (8 bp) and CDEIII (28 bp) (13, 39). Mutational analyses indicate that while CDEI and CDEII both contribute to optimal centromere function (14, 18, 19, 39), CDEIII is essential for function (15, 34, 40).

A protein (CP1, CPF1, or CBF1) that binds to CDEI has been identified (1, 7, 31). Disruption of the gene encoding this protein causes pleiotropic effects, including a 10-fold increase in mitotic chromosome missegregation (2, 8, 36). A multisubunit protein complex (CBF3) that binds to CDEIII has been characterized (33). Recently, this complex was shown to interact with microtubules in vitro and to contain a minus-end-directed microtubule-based motor (28).

While much is known about yeast centromere DNA and the major structural components of the mitotic spindle (26), comparatively little is known about the *trans*-acting factors involved in chromosome movement. A number of genetic strategies have been used to obtain yeast mutants defective in chromosome segregation. For instance, chromosome transmission fidelity (*ctf*) mutants were isolated by screening for missegregation of a marked chromosome fragment (56). The chromosome instability genes *CIN1*, *CIN2*, and *CIN4* were identified because some mutant alleles cause supersensitivity to microtubule-depolymerizing drugs and increased mitotic chromosome loss (24, 57). Many factors affect the efficiency of chromosome segregation. For example, Hartwell and Smith (21) showed that 13 of 14 cell division cycle mutants tested exhibited an increase in chromosome loss. In fact, mutations in several genes involved in various stages of the cell cycle have been shown to increase chromosome missegregation (41). Therefore, it is expected that a simple chromosome loss screen will yield many mutations that indirectly affect chromosome segregation.

The strategy we used to isolate chromosome segregation mutants is based on monitoring a marked copy of chromosome III in which the wild-type centromere has been replaced by a partially functional mutant centromere, *cen3X69* (Fig. 1) (35). We predicted that the *cen3X69* centromere would make transmission of the marked chromosome particularly sensitive to mutations which affect the segregation machinery. Furthermore, the *cen3X69* centromere could allow us to isolate mutants exhibiting synthetic phenotypes that result from interactions between mutant DNA and mutant proteins (26). Here we report the isolation of two new cold-sensitive chromosome segregation mutants, *cse1* and *cse2*, and describe the cloning, characterization, and disruption of the *CSE1* and *CSE2* genes. We present evidence that these genes encode proteins that function in mitosis and have important roles in ensuring high-fidelity chromosome segregation in *S. cerevisiae*.

MATERIALS AND METHODS

Media, strains, and DNA manipulations. Media for yeast growth and sporulation were described previously (35). Color medium contains 0.6% Difco yeast nitrogen base, 0.5% Casamino Acids, 2% glucose, 50 μg of tryptophan per

* Corresponding author.
† Present address: Dana-Farber Cancer Institute and Harvard Medical School, Boston, MA 02115.
‡ Present address: Immunex Corporation, Seattle, WA 98101.

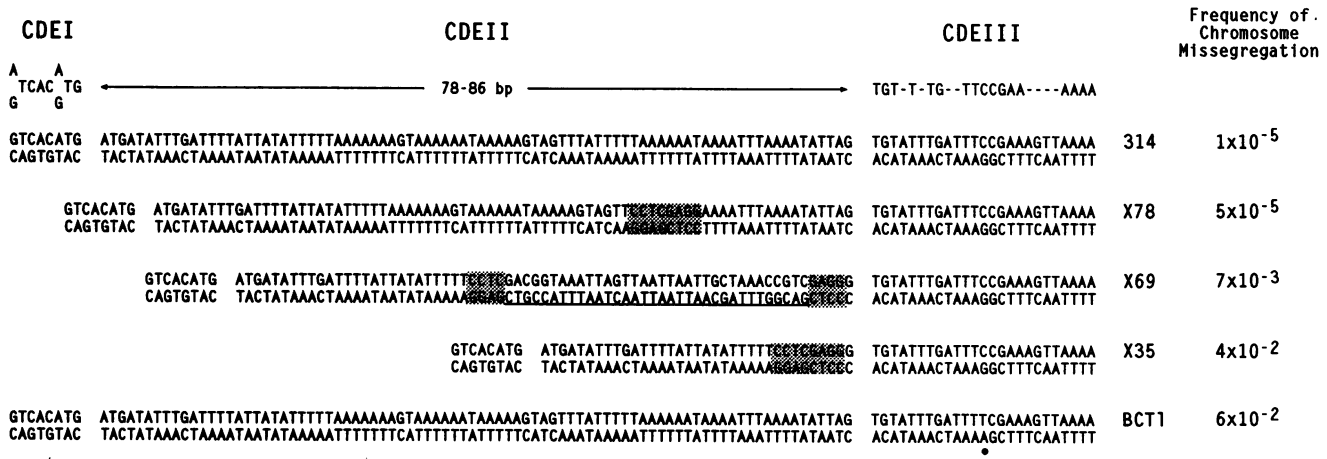

FIG. 1. DNA sequences of centromeres used in this study. The organization of CDEI, CDEII, and CDEIII is shown at the top. The CDEI and CDEIII consensus sequences represent nucleotide positions that are conserved in the 12 *S. cerevisiae* centromere DNAs analyzed to date. The *CEN314* centromere is a fully functional derivative of wildtype *CEN3* DNA (34). The shaded areas indicate the positions of the *Xho*I linkers (CCTCGAGG). The 34-bp oligonucleotide insertion into the *Xho*I site is underlined in *cen3X69* (18). The black dot indicates the position of the C-to-T mutation in *cen3BCT1* (34). The missegregation frequency of chromosome III carrying the indicated centromere is presented on the right as the number of segregation errors per cell division.

ml, 30 μg of uracil per ml, and 5 μg of adenine per ml (23). 5-Fluoro-orotic acid (5-FOA) medium contains 0.5 mg of 5-FOA (PCR Inc., Gainesville, Fla.) per ml in minimal medium supplemented with 20 μg of uracil per ml and other nutrients as necessary (5). The yeast strains used in this study are listed in Table 1. Genetic analysis was performed by standard protocols (51). Meiotic mapping data were analyzed with Tetrads software (provided by J. King). All yeast strains were grown at 30°C unless otherwise stated. Gel-purified DNA fragments were ^{32}P labeled with an oligonucleotide-labeling kit (Pharmacia) according to the manufacturer's instructions. Labeled DNA fragments were purified over a Sephadex G-50 column, and about 10^6 cpm was used in each hybridization reaction. All enzymes were purchased from New England BioLabs, Inc. (Beverly, Mass.), and used as specified by the company.

EMS mutagenesis and mutant isolation. The disomic strain 41-14d (35), which contains one native chromosome III and one copy of chromosome III (the *X69* chromosome) bearing the mutant centromere (*cen3X69*), *URA3*, and *SUP11*, was mutagenized with ethyl methanesulfonate (EMS; Kodak) to 2 to 10% cell survival. After mutagenesis, the cells were plated on color medium and incubated for 5 days at 30°C. Yeast colonies exhibiting many red and white sectors were streaked onto color medium to confirm the high-sectoring phenotype. Putative high-sectoring isolates were tested for growth at 15°C.

To eliminate additional *cis*-acting mutations in the *cen3X69* centromere, haploid red colonies that had lost the *X69* chromosome were mated with 415F1X69. The resulting diploid colonies were sporulated, and the asci were dissected. Twenty complete tetrads from each cross were tested, and in all cases the cold-sensitive phenotype showed $2^+:2^-$ segregation. To determine whether the cold-sensitive and high-sectoring phenotypes cosegregate, reciprocal matings were performed to construct diploid strains homozygous for the cold-sensitive alleles but heterozygous at *CEN3* (*CEN3/cen3X69-URA3-SUP11*; e.g., Y1705 × Y1707). Strains heterozygous for both the cold-sensitive and *CEN3* alleles were also constructed as controls (e.g., Y1706 × Y1707). The resulting diploids were then streaked onto color medium plates, and the high-sectoring phenotypes were scored after 5 days at 30°C. Four successive crosses and genetic analyses of the meiotic products were performed for each mutant.

Strains and assays used to measure chromosome segregation. Haploid *cse* strains carrying *SUP11*-marked chromosomes with mutant centromeres (*cen3-URA3-SUP11*) were obtained either by one-step gene replacement or by crossing appropriate meiotic segregants derived from heterozygous diploids. Strains Y1719 (*CEN314* chromosome), Y1720 (*X35* chromosome), and Y1721 (*BCT1* chromosome) were constructed by transforming Y1705 (*cse1-1*) with *Eco*RI-cut pJUP314, pJUPX35, or pJUPBCT1 DNA, respectively (35). Strain Y1722 (*X78* chromosome) is a haploid segregant from a diploid formed by crossing Y1705 (*cse1-1*) with 415F1X78 (19). Homozygous *cse1-1* diploids containing one copy of a *SUP11*-marked chromosome III were constructed by the crosses Y1705 × Y1707, Y1720 × Y1709, Y1721 × Y1709, and Y1722 × Y1705 and used in colony color assays. Haploid *cse2-1* strains containing *SUP11*-marked chromosomes with mutant centromeres were obtained by crossing Y2009 (*cse2-1*) with 415F1314, 415F1X78, or 415F1X35. Homozygous *cse2-1* diploid strains with one *SUP11*-marked chromosome III were obtained from the following crosses: Y2009 × Y2028, Y2009 × Y2030, and Y2009 × Y2031.

The mitotic segregation of *SUP11*-marked chromosomes carrying mutant centromeres (*cen3-URA3-SUP11*) was measured by a colony color assay (23) which uses the dose-dependent suppression by *SUP11* of an *ade2-101* ochre mutation to create a visual signal for chromosome number. Diploid cells (*ade2-101/ade2-101*) with zero, one, or two or more copies of *SUP11* form red, pink, or white colonies, respectively. In each assay, two to four pink colonies (or sectoring colonies in cases of frequent chromosome missegregation) were picked from color medium, and about 200 cells per plate were spread onto color medium plates (150 by 15 mm) and incubated for 4 days at 30°C and then overnight at 4°C. Half-sectored colonies, indicating a chromosome missegregation event in the first cell division after plating, were counted (23). The number of red-and-pink half-sectored colonies divided by the total number of pink colonies is

TABLE 1. Yeast strains used in this study

Name	Genotype	Source
41-14d	*MATa/MATα cen3X69-URA3-SUP11/CEN3 ura3-52 ade2-101 lys2-801 trp1Δ-901*	Our laboratory
415F1314	*MATa ura3-52 CEN314-URA3-SUP11 ade2-101 leu2-3,112 his3-11,15*	Our laboratory
415F1X78	*MATa ura3-52 cen3X78-URA3-SUP11 ade2-101 leu2-3,112 his3-11,15*	Our laboratory
415F1X69	*MATa ura3-52 cen3X69-URA3-SUP11 ade2-101 lys2-801 trp1-Δ901 leu2-3,112 his3-11,15*	Our laboratory
415F1X35	*MATa ura3-52 cen3X35-URA3-SUP11 ade2-101 trp1-Δ901 leu2-3,112 his3-11,15*	Our laboratory
MM1401	*MATa/MATα ade2-101/ADE2 can1/CAN1 his3-Δ200/his3-Δ200 leu2-Δ1/leu2-Δ1 ura3-52/ura3-52 lys2-801/lys2-801 trp1-Δ101/trp1-Δ101*	J. Woolford
YS28	*MATα cir⁺ ura3 his2 leu1 lys1 met4 pet8*	M. Fournier
YS138	*MATα prp2-1 leu2 his7 ade1 lys2*	M. Fournier
YP3a	*MATa ura3-52 ade2-101 lys2*	P. Hieter
Y1705	*MATα ura3-52 ade2-101 his3-11,15 trp1-Δ901 cse1-1*	This study
Y1706	*MATα ura3-52 ade2-101 his3-11,15 trp1-Δ901*	This study
Y1707	*MATa cen3X69-URA3-SUP11 ura3-52 leu2-3,112 his3-11,15 ade2-101 trp1-Δ901 cse1-1*	This study
Y1709	*MATa ura3-52 ade2-101 his3-11,15 trp1-Δ901 cse1-1*	This study
Y1718	*MATa/MATα ura3-52/URA3 cse1-1/cse1-1*	This study
Y1719	*MATα ura3-52 CEN314-URA3-SUP11 ade2-101 his3-11 trp1-Δ901 cse1-1*	This study
Y1720	*MATα ura3-52 cen3X35-URA3-SUP11 ade2-101 his3-11 trp1-Δ901 cse1-1*	This study
Y1721	*MATα ura3-52 cen3BCT1-URA3-SUP11 ade2-101 his3-11 trp1-Δ901 cse1-1*	This study
Y1722	*MATa ura3-52 cen3X78-URA3-SUP11 ade2-101 his3-11 trp1-Δ901 cse1-1*	This study
Y1729	*MATa/MATα ura3-52/ura3-52 CEN3/CEN314-URA3-SUP11 ade2-101/ade2-101 trp1-Δ901/trp1-Δ901 his3-11,15/his3-11,15 cse1-1/cse1-1*	This study
Y2006	*MATa cen3X69-URA3-SUP11 ura3-52 leu2-3,112 his3-11,15*	This study
Y2008	*MATa ura3-52 ade2-101 his3-11,15 trp-1Δ901 cse2-1*	This study
Y2009	*MATα ura3-52 ade2-101 his3-11,15 trp1-Δ901 cse2-1*	This study
Y2014	*MATa/MATα ura3-52/URA3 cse2-1/cse2-1*	This study
Y2018	*MATa/MATα ura3-52/ura3-52 CEN3/CEN314-URA3-SUP11 ade2-101/ade2-101 trp1-Δ901/trp1-Δ901 his3-11,15/his3-11,15 cse2-1/cse2-1*	This study
Y2028	*MATa ura3-52 CEN314-URA3-SUP11 ade2-101 his3-11 trp1-Δ901 cse2-1*	This study
Y2030	*MATa ura3-52 cen3X78-URA3-SUP11 ade2-101 his3-11 trp1-Δ901 cse2-1*	This study
Y2031	*MATa ura3-52 cen3X35-URA3-SUP11 ade2-101 his3-11 trp1-Δ901 cse2-1*	This study
M1702	*MATa/MATα cse1::LEU2/CSE1 ade2-101/ADE2 can1/CAN1 his3-Δ200/his3-Δ200 leu2-Δ1/leu2-Δ1 ura3-52/ura3-52 lys2-801/lys2-801 trp1-Δ101/trp1-Δ101*	This study
M2002	*MATa cse2::HIS3 can1 leu2-3,112 his3-Δ200 ura3-52 trp1-Δ101 lys2-801*	This study
M2003	*MATα cse2::HIS3 ade2-101 leu2-3,112 his3-Δ200 ura3-52 trp1-Δ101 lys2-801*	This study
M2039	*MATα prp2-1 his3 leu2 can1 lys2*	This study
M2046	*MATa pet8 trp1 his3 leu1 leu2*	This study
M2055	*MATa/MATα cse2::LEU2/CSE2 ade2-101/ADE2 can1/CAN1 his3-Δ200/his3-Δ200 leu2-Δ1/leu2-Δ1 ura3-52/ura3-52 lys2-801/lys2-801 trp1-Δ101/trp1-Δ101*	This study
M2056	*MATa can1 leu2-3,112 trp1-Δ101 his3-Δ200 ura3-52 lys2-801 cse2::LEU2*	This study
H1709	*MATα ura3-52 orf2::URA3 ade2-101 his3-11,15 trp1-Δ901 cse1-1*	This study

the chromosome loss frequency (1:0 segregation), and the number of red-and-white half-sectored colonies divided by the total number of pink colonies is the chromosome nondisjunction frequency (2:0 segregation). For strains with very unstable chromosomes, the number of half-sectored colonies divided by the total number of white-and-pink sectoring colonies represents the minimum frequency of chromosome missegregation.

The number of Ura$^-$ cells resulting from the infrequent nondisjunction or loss of chromosomes with wild-type centromeres was determined with 5-FOA (5). Diploid *cse1-1* or *cse2-1* strains heterozygous for *URA3* (Y1718, Y1729, Y2014, and Y2018) were constructed by crossing appropriate haploid strains. Cells were grown overnight in selective medium lacking uracil, and approximately 10^6 cells were plated on 5-FOA plates (150 by 15 mm). In parallel, 100 cells were spread on each yeast extract-peptone-dextrose (YEPD) plate and counted after 2 days of incubation at 30°C to measure viability. The missegregation frequency was calculated as the total number of Ura$^-$ colonies divided by the total number of viable cells. In both the colony color and 5-FOA assays, at least three independent experiments, each with three parallel samples, were performed. In each case, more than 200 colonies were counted, and the data were subjected to statistical analysis (54).

Mitotic recombination. Some recombination events produce Ura$^-$ cells that are phenotypically identical to cells generated by chromosome missegregation events. For instance, reciprocal mitotic recombination between *URA3* (adjacent to *CEN314*) and *MAT* followed by loss of the *URA3* chromosome results in aneuploid ($2n - 1$) Ura$^-$ Sup$^-$ cells that can mate with a tester strain. Gene conversion of *CEN314-URA3-SUP11* to *CEN3* without chromosome loss results in Ura$^-$ Sup$^-$ cells that are nonmaters. We determined the frequency of mitotic recombination between *URA3* and *MAT* for Ura$^-$ cells generated by strains homozygous for *cse1* or *cse2* in which one of the two chromosome III copies carried *URA3* (e.g., Y1719 × Y1709 or Y2028 × Y2009). Although not all recombination events occurring in the interval were measured, these results would indicate any significant differences in mitotic recombination frequencies between the wild-type and mutant strains.

Four colonies picked from selective plates lacking uracil were diluted in water; 100 cells were plated on each of three YEPD plates (for cell viability), and 10^6 cells were plated on each of three 5-FOA plates and incubated for 3 days at 30°C.

Cells were patched onto appropriate plates to confirm the Ura^- and Sup^- phenotypes and then tested for mating type (51). At least 100 Ura^- colonies for each sample were analyzed in each of two independent experiments. The mitotic recombination frequency was calculated as the total number of Ura^- Sup^- cells able to mate with *MATα* haploids or unable to mate divided by the total number of viable cells.

Cellular and nuclear morphology. Yeast strains were grown to a density of about 10^6 cells per ml at 30°C in liquid YEPD and then shifted to 11°C for 48 h. Cells collected at 0, 24, and 48 h were briefly sonicated, and the cellular morphologies were examined by phase-contrast microscopy. The numbers of unbudded, small-budded (bud less than half the diameter of the mother cell), large-budded (bud greater than half the diameter of the mother cell) and abnormal (multiple buds or very elongated, swollen buds) cells were determined by counting at least 200 cells for each sample at each time point. The DNA was visualized by staining with DAPI (4′,6′-diamidino-2-phenylindole; Sigma).

Cloning *CSE1* and *CSE2*. *Escherichia coli* DH5αF′ [F′ *endA1 hsdR17* (r_K^- m_K^+) *supE44 thi-1 recA1 gyrA96*(Nal^r) *relA1* Δ(*lacZYA-argF*)*U169* φ80d*lac*Δ(*lacZ*)M15] was used for all plasmid manipulations. A low-copy-number yeast genomic YCp50 library (American Type Culture Collection) was used to transform Y1705 (*cse1-1*) or Y2009 (*cse2-1*) cells by the lithium acetate method (51). Ura^+ transformants were restreaked for single colonies to confirm wild-type growth at 15°C and crossed with *cse1-1* (Y1707) or *cse2-1* (Y2006) haploid strains carrying the *X69* chromosome to visualize the sectoring phenotypes on color medium plates. Plasmids that rescue the cold-sensitive phenotype of Y1705 (*cse1-1*) or Y2009 (*cse2-1*) were recovered from *S. cerevisiae* by transforming *E. coli*. DNA fragments were subcloned into the appropriate pRS vectors (52) for functional analyses.

DNA sequencing and computer analysis. DNA sequences were determined by the dideoxynucleotide-chain termination method with the T7 double-stranded sequencing procedure (Pharmacia). Fragments of yeast DNA were inserted into the polylinker regions of the pRS vectors to permit direct sequencing of both strands (52). Oligonucleotides designed from new sequences were used as primers in subsequent sequencing reactions.

Nucleic and amino acid sequences were analyzed with GCG software (Genetics Computer Group, Inc.; version 7.1) on a Sun Microsystems Sparcstation. Data bases (GenBank, release 73.0; EMBL, release 32.0; Swiss Protein, release 23.0; and Prosite, release 9.2) were searched with the FASTA, TFASTA, and Wordsearch programs. Potential promoter elements, transcription termination sequences, nuclear localization signals, and the *CSE2* bZIP region were determined by visual inspection. DNA sequences were manipulated with DNA Inspector IIe and the Gene Construction Kit (Textco, Inc., Lebanon, N.H.) on a Macintosh computer.

Disruption of *CSE1* and *CSE2*. *CSE1* was disrupted by replacing the 164-bp *Bgl*II fragment in the coding region with a 3-kb *Bgl*II fragment containing *LEU2* (Fig. 2A). The resulting plasmid, p1720, was digested with *Pst*I and used to transform yeast strain MM1401 to Leu^+. The disrupted allele in M1702 (*cse1*::*LEU2*/*CSE1*) was confirmed by Southern hybridization (data not shown).

CSE2 was disrupted by inserting a 1.8-kb *Bam*HI *HIS3* fragment into the unique *Bam*HI site (Fig. 2B). The resulting plasmid, p2017, was cut with *Sal*I and used to transform MM1401 to His^+. The disrupted allele in the heterozygous *cse2*::*HIS3*/*CSE2* strain was confirmed by Southern hybridization (data not shown), and a haploid segregant, M2002 (*cse2*::*HIS3*), was used for meiotic mapping. Because the *HIS3* fragment contains promoter sequences that could be used to express a fusion protein in *S. cerevisiae*, *CSE2* was also disrupted by inserting a 3-kb *Bgl*II *LEU2* fragment into the *Bam*HI site. The resulting plasmid, p2020, was cut with *Xba*I and *Sph*I (in the pRS polylinker) and used to transform MM1401 to Leu^+. The disrupted allele in M2055 (*cse2*::*LEU2*/*CSE2*) was confirmed by Southern hybridization (data not shown).

Mapping *CSE1* and *CSE2*. Chromosome mapping was performed (11) with a yeast strain in which chromosome VII is split into two chromosome fragments at *RAD2* (provided by P. Hieter). Chromosome separation gels were transferred to nitrocellulose membranes and hybridized with either a 7-kb *Bam*HI-*Apa*I *CSE1* fragment or a 0.4-kb *Cla*I-*Bam*HI *CSE2* fragment (Fig. 2).

To confirm that the cloned DNA contained the cognate *CSE1* allele, *URA3* was inserted between the *Eco*RI and *Sma*I sites in unidentified open reading frame 2 (*ORF2*) (Fig. 2A). The resulting plasmid (p1719) was cut with *Bam*HI and *Sal*I (in the pRS314 polylinker) and used to transform Y1705 (*cse1-1*) to Ura^+. The transformed haploid was crossed with YP3a, and the resulting diploid strain was sporulated. Analysis of the haploid products demonstrated that *cse1-1* and *URA3* are linked in this strain (H1709).

Meiotic mapping of the *cse2*::*HIS3* allele was performed with the following crosses: M2002 (*cse2*::*HIS3*) × M2039 (*prp2-1*), M2003 (*cse2*::*HIS3*) × M2046 (*pet8*), and M2003 × 415F1314. M2039 is a meiotic segregant obtained by crossing M2002 with YS138 (*prp2-1*), and M2046 is a meiotic segregant obtained by crossing M2002 with YS28 (*pet8 his2*). The cold-sensitive allele (*cse2-1*) was mapped with respect to the temperature-sensitive allele (*prp2-1*) by crossing M2039 with Y2008 (*cse2-1*).

Nucleotide sequence accession numbers. The nucleotide sequences of the *CSE1* and *CSE2* genes have been deposited in GenBank under accession numbers L14838 and L14839, respectively.

RESULTS

Isolation of cold-sensitive chromosome segregation mutants. Yeast strain 41-14d, which contains one native chromosome III and one copy of the *X69* chromosome, forms white colonies with occasional red sectors resulting from missegregation of the *X69* chromosome. Approximately 40,000 colonies were screened after mutagenesis of 41-14d, and 694 colonies that sectored more than the parent disome were picked. Fifteen of these exhibited reproducible cold-sensitive phenotypes, but only 2 of the 15 strains (cs17 and cs20) exhibited cosegregation of the cold-sensitive and high-sectoring phenotypes. The cs17 and cs20 strains were subjected to four successive crosses to eliminate possible multiple mutations (Materials and Methods). After the final cross, the high-sectoring and cold-sensitive phenotypes cosegregated in more than 50 complete tetrads, indicating that for each mutant the two phenotypes are caused by a mutation in a single gene. These two chromosome segregation (*cse*) mutants were designated *cse1* and *cse2*, and the mutant alleles were named *cse1-1* and *cse2-1*, respectively.

***cse1-1* and *cse2-1* increase chromosome missegregation.** We found that the frequencies of nondisjunction and loss of the *X69* chromosome were 51-fold higher in *cse1-1*/*cse1-1* strains and 8-fold higher in *cse2-1*/*cse2-1* strains than in wild-type strains (Table 2). We also analyzed chromosomes bearing

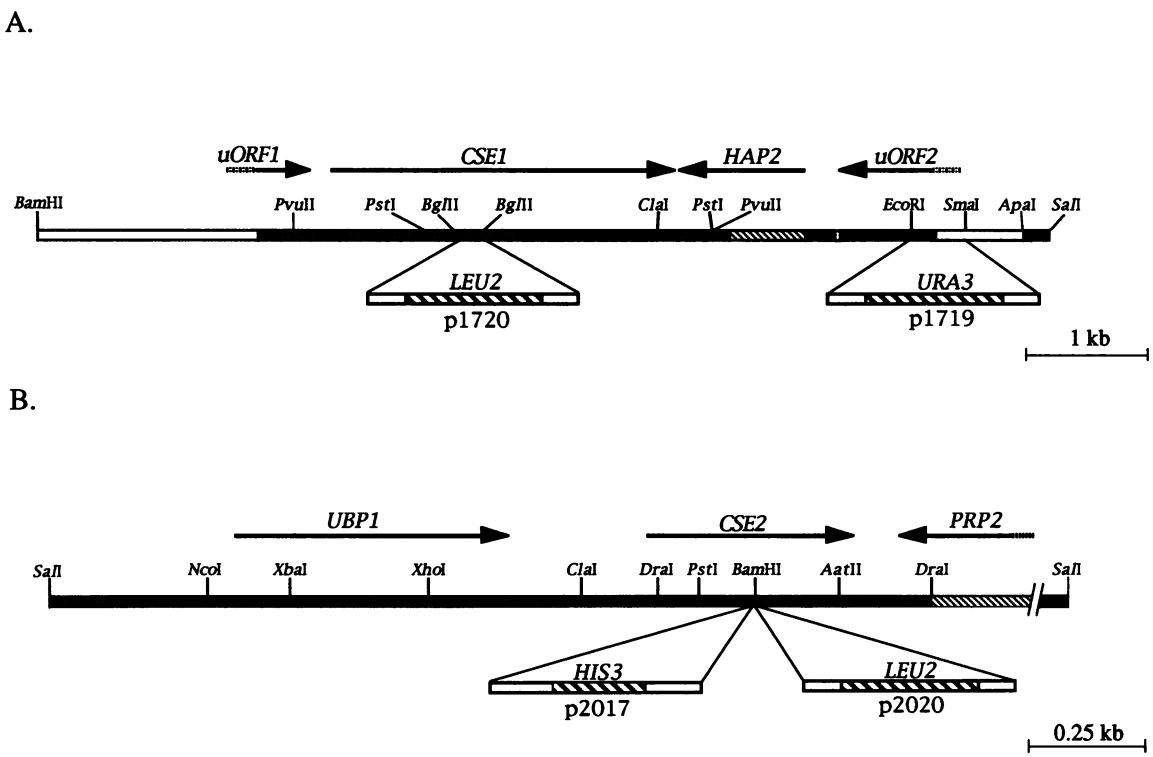

FIG. 2. Genomic organization of *CSE1* and *CSE2*. (A) The shaded regions of the map indicate DNA that was sequenced, the open segments indicate regions that were not sequenced, and the solid black region shows vector sequences. The hatched region of the map depicts the overlap with published *HAP2* sequences (44). The arrows show the directions of transcription of *CSE1*, *HAP2*, and the unidentified ORFs (uORF). The positions of the *LEU2* (p1720) and *URA3* (p1719) insertions and the *Pvu*II sites used to construct p314P3.5 are indicated. Not all restriction sites are shown. (B) The shaded region of the map indicates DNA that was sequenced, the hatched region indicates the overlap with published *PRP2* sequences (9), and the solid black region shows vector sequences. About 400 bp of *PRP2* and 300 bp of YCp50 vector DNA are not shown, as indicated by the break between the hatched and solid regions. The arrows indicate the directions of transcription of *CSE2*, *PRP2*, and the upstream basic protein gene (*UBP1*). The positions of the *LEU2* (p2020) and *HIS3* (p2017) insertions into *CSE2* are indicated. Not all restriction sites are shown.

other mutant centromeres (Fig. 1) to determine if the segregation defects were specific for the *cen3X69* mutation. The missegregation frequencies of the *X35* and *BCT1* chromosomes in *cse1-1/cse1-1* strains (6.8×10^{-1} and 6.9×10^{-1}, respectively) and of the *X35* chromosome in *cse2-1/cse2-1* strains (4.9×10^{-1}) are comparable to those exhibited by acentric chromosomes in wild-type strains (Table 2) (12). Missegregation of the *X78* chromosome increased more than 100-fold in *cse1-1/cse1-1* strains, mostly because of a high frequency of chromosome nondisjunction events. This is particularly surprising, since the *cen3X78* mutation alone increases missegregation by only about fivefold in comparison with *CEN3* in wild-type strains (18). In contrast, no increase in missegregation was detected for the *X78* chromosome in *cse2-1* homozygotes (Table 2).

Segregation of the *X78*, *X69*, and *X35* chromosomes was the same in heterozygous *cse* strains (*cse1-1/CSE1* and *cse2-1/CSE2*) as in wild-type strains, indicating that the *cse1-1* and *cse2-1* mutations are recessive with regard to the chromosome segregation defect (Table 2). A statistically significant increase in aberrant segregation of the *BCT1* chromosome was detected in heterozygous *cse1-1/CSE1* cells but not in heterozygous *cse2-1/CSE2* cells, indicating that the *cse1-1* mutation is partially dominant with respect to the function of the *BCT1* centromere (Table 2).

***cse* mutations cause more chromosome nondisjunction than loss.** In both of the homozygous *cse1-1* and *cse2-1* strains, the number of segregation errors was low enough for nondisjunction and loss events to be differentiated by the colony-sectoring assay. For these strains, we found that the frequency of nondisjunction was higher than the frequency of loss (Table 2). In *cse1-1/cse1-1* strains, nondisjunction events involving the *X78* chromosome were 13 times more frequent than loss events. In *cse2-1/cse2-1* strains, nondisjunction events involving the *X69* chromosome were 27 times more frequent than loss events. Therefore, while the *cse1-1* and *cse2-1* alleles cause both loss and nondisjunction, in at least two strains the predominant effect of these mutations is an increase in chromosome nondisjunction.

cse* mutations have little effect on wild-type centromeres, do not increase mitotic recombination, and cause intermediate sensitivity to nocodazole.** The *cse* mutations have relatively small effects on the segregation of chromosomes with wild-type centromeres. The frequency of missegregation of chromosomes V and III increased no more than 14-fold in *cse1-1/cse1-1* and *cse2-1/cse2-1* strains (Table 3). Recombination frequencies for the interval between *URA3* (adjacent to the centromere) and *MATa** were not significantly higher in the *cse1-1/cse1-1* and *cse2-1/cse2-1* diploid strains than in the wild type (Table 3).

The chromosome missegregation phenotype prompted us to test the *cse* mutants for sensitivity to the microtubule-depolymerizing drug nocodazole. We found that wild-type cells grew on plates containing 7.5 μg of nocodazole per ml

TABLE 2. Segregation of chromosome III derivatives with mutant centromeres in *cse* strains

Genotype	Missegregation frequency (10^{-3}) (mean ± SD)[a]											
	cen3X78			*cen3X69*			*cen3X35*			*cen3BCT1*		
	CND	CHL	Total	CND	CHL	Total	CND	CHL	Total	CND	CHL	Total
WT[b]/WT	NA	NA	<0.6 (1)	5.8 ± 0.9 (1)	1.0 ± 0.1 (1)	6.8 (1)	24 ± 6 (1)	12 ± 4.1 (1)	36 (1)	57 ± 21 (1)	8.6 ± 0.4 (1)	66 (1)
cse1-1/CSE1	NA	NA	<0.6 (1)	6.4 ± 4.9 (1.1)	2.5 ± 2.4 (2.5)	8.9 (1.3)	30 ± 6 (1.3)	6.5 ± 2.6 (0.5)	36.5 (1)	ND	ND	130 ± 10 (2)
cse1-1/cse1-1	64 ± 40	4.8 ± 3.5	69 (>108)	ND	ND	350 ± 140 (51)	ND	ND	680 ± 100 (19)	ND	ND	690 ± 20 (10)
cse2-1/CSE2	NA	NA	<0.6 (1)	4.0 ± 3.7 (0.7)	2.2 ± 0.9 (2.2)	6.2 (0.9)	23 ± 15 (1)	8.7 ± 5.6 (0.7)	31.7 (0.9)	60 ± 2 (1)	11 ± 8.5 (1.3)	71 (1)
cse2-1/cse2-1	NA	NA	<0.5 (1)	55 ± 18 (9.5)	2.0 ± 0.1 (2)	57 (8.4)	ND	ND	490 ± 90 (14)	NP	NP	NP

[a] All strains are diploids containing one copy of the *SUP11*-marked chromosome III with the indicated mutant centromere and one copy of chromosome III with wild-type *CEN3*. Chromosome nondisjunction (CND) and chromosome loss (CHL) frequencies were measured by the colony color assay. The numbers in parentheses represent the fold increase relative to wild-type backgrounds. NA, not assayable (sectoring not frequent enough to measure by the colony color assay); ND, not distinguishable (sectoring too frequent to distinguish CND from CHL events), so the total missegregation frequencies are reported; NP, not possible to construct stable *cse2-1* homozygotes containing the *BCT1* chromosome.
[b] WT, wild type.

TABLE 3. Mitotic chromosome missegregation and recombination frequencies in *cse* strains

Relevant genotype	Total missegregation frequency (10^{-4}) (mean ± SD) on chromosome[a]:		Recombination frequency (10^{-5}) (*CEN3/MAT*)[b]
	V	III	
WT[c]/WT	0.53 ± 0.14 (1)	1.2 ± 0.5 (1)	1.4
cse1-1/CSE1	0.66 ± 0.46 (1.2)	3.0 ± 2.4 (2.5)	0.4
cse1-1/cse1-1	5.5 ± 2.1 (10)	17 ± 7 (14)	<1[d]
cse2-1/CSE2	0.64 ± 0.43 (1.2)	2.9 ± 2.5 (2.4)	2
cse2-1/cse2-1	1.6 ± 0.6 (3.0)	3.9 ± 3.8 (3.3)	1.3

[a] The total number of mitotic chromosome missegregation events (chromosome loss plus chromosome nondisjunction) was measured by the 5-FOA assay. Numbers in parentheses are normalized to wild-type (CSE^+/CSE^+) backgrounds.
[b] Mitotic recombination events in the interval between *MAT* and *URA3* were determined as described in Materials and Methods, and the data reported here are the means from three independent experiments.
[c] WT, wild type.
[d] No recombination events were detected among the 226 Ura^- colonies screened.

but that *cse1-1* cells did not grow and *cse2-1* cells grew only slowly at this concentration (data not shown). The *cse1-1* cells were able to grow on 5 μg of nocodazole per ml. In contrast, the *tub* (*tub1-1* and *tub2-403*) and *cin* (*cin1*::*HIS3*, *cin2*::*LEU2*, and *cin4*::*URA3*) mutants we tested could not grow until the concentration of nocodazole was reduced to 1 μg/ml.

Cloning and mapping of *CSE1* and *CSE2*. Five plasmids containing overlapping DNA fragments that rescue both the cold-sensitive and high-sectoring phenotypes exhibited by Y1705 (*cse1-1*) were isolated from the YCp50 library. Subcloning and complementation studies showed that the functional region spanned a *Cla*I site (Fig. 2A). Subsequently, a 3.5-kb *Pvu*II fragment containing only *CSE1* (p314P3.5) was shown to complement the cold-sensitive and high-sectoring phenotypes caused by *cse1-1* (Fig. 2A).

Hybridization of the 7-kb *Bam*HI-*Apa*I fragment (Fig. 2A) to separated yeast chromosomes indicates that *CSE1* is located on chromosome VII. DNA sequencing revealed that *CSE1* is adjacent to *HAP2*, which was previously mapped to the left arm of chromosome VII (44). Integrative transformation was used to insert *URA3* into a region about 2 kb from the *cse1-1* allele in order to confirm that *CSE1*, and not a suppressor gene, had been cloned (Fig. 2A and Materials and Methods). Genetic analysis revealed that *URA3* and

TABLE 4. Meiotic mapping

Genetic markers	Segregation ratio[a]		Distance (cM)[b]
	FDS:SDS	PD:NPD:TT	
cse1-1-orf2::*URA3*		53:0:3	2.7
cse2::*HIS3-trp1*	85:7		3.9
cse2::*HIS3-CEN3*	87:6		3.3
cse2::*HIS3-pet8*		68:0:4	2.8
cse2::*HIS3-prp2-1*[c]		32:0:4	5.6
CEN14-pet8[d]	605:17		
cse2-1-prp2-1[c]	19:0		

[a] PD, parental ditype; NPD, nonparental ditype; TT, tetratype; FDS, first-division segregation; SDS, second-division segregation.
[b] Map distances in centimorgans (cM) were calculated by the formula 100[(TT + 6NPD)/2(PD + NPD + TT)] (37) and by a Macintosh tetrad analysis program provided by J. King.
[c] *prp2-1* causes temperature sensitivity at 32°C.
[d] The *CEN14-pet8* data are taken from reference 38.

cse1-1 are tightly linked in this strain (Table 4), demonstrating that the cloned DNA contains the authentic *CSE1* allele.

Two overlapping plasmids that rescue the cold-sensitive and high-sectoring phenotypes exhibited by Y2009 (*cse2-1*) were isolated from the YCp50 library. Subsequent analyses indicated that the rescuing activity spans a *Bam*HI site (Fig. 2B). A 1.8-kb *Cla*I-*Sal*I fragment containing *CSE2* was cloned into pRS316 and shown to complement both the cold-sensitive and high-sectoring phenotypes of Y2009 (Fig. 2B).

Hybridization of the 0.4-kb *ClaI-Bam*HI fragment (Fig. 2B) to a chromosome blot indicated that *CSE2* is located on chromosome XIV. Genetic mapping to further position *CSE2* on this chromosome was performed by crossing *cse2::HIS3* mutants with strains bearing genetic markers on chromosome XIV. The meiotic mapping data shown in Table 4 indicate that the *CSE2* gene is located on the right arm about 3 centimorgans from *CEN14*. The linkage between *cse2-1* and *prp2-1* was confirmed by analyzing the meiotic products obtained from crossing Y2008 (*cse2-1*) with M2039 (*prp2-1*) (Table 4). Subsequent DNA sequence analysis showed that *CSE2* is adjacent to *PRP2* (Fig. 4) (9). These results, together with published genetic data (38), indicate that the likely order of these genetic loci is *CEN14-pet8-cse2-prp2*.

Southern hybridization showed that *CSE1* and *CSE2* are single-copy genes in *S. cerevisiae*. Northern analysis revealed a 3-kb *CSE1*-specific RNA and a 0.5-kb *CSE2*-specific RNA in both total and poly(A)$^+$ RNA preparations (data not shown).

***CSE1* and *CSE2* encode novel proteins.** About 4 kb of the 7-kb *Bam*HI-*Apa*I region was sequenced and found to contain four potential ORFs (Fig. 2A). Computer searches failed to reveal any genes or proteins with significant homology to *CSE1*, *ORF1*, or *ORF2*. However, the ORF immediately downstream from *CSE1* was identified as *HAP2* (44). We know that the chromosome segregation defect exhibited by *cse1-1* cells is not caused by a mutation in *HAP2*, *ORF1*, or *ORF2* because the 3.5-kb *Pvu*II fragment containing only *CSE1* can complement both the cold-sensitive and high-sectoring phenotypes (Fig. 2A). The 2,880-bp *CSE1* ORF encodes a putative 960-amino-acid protein with a calculated molecular weight of 109,230 and a charge of −28 at pH 7.0. The protein contains 43% hydrophobic amino acids and has a possible bipartite nuclear localization sequence (Fig. 3) (16). The carboxy-terminal 48 amino acids, the 3′ untranslated region, or both are essential for CSE1 function, since a truncated *CSE1* gene lacking sequences downstream from the *Cla*I site is unable to complement the cold-sensitive phenotype of *cse1-1* cells. Codon usage in the *CSE1* ORF suggests that this gene product is expressed at low levels (50).

Sequence analysis of 2.8 kb of yeast genomic DNA that complemented the *cse2-1* cold-sensitive phenotype revealed two complete ORFs, one encoding CSE2 and another encoding an unknown upstream basic protein (UBP1 [Fig. 2B]). Computer searches revealed that both ORFs are predicted to encode novel proteins. The 1.8 kb *Cla*I-*Sal*I fragment containing *CSE2* but not *UBP1* was shown to complement the cold-sensitive and high-sectoring phenotypes exhibited by *cse2-1* cells (Fig. 2B). Haploid cells with the *UBP1* gene disrupted were viable, indicating that the *UBP1* gene is not essential for growth (data not shown). The 447-bp *CSE2* ORF is predicted to encode a 149-amino-acid protein with a calculated molecular weight of 17,357 and a charge of −3 at pH 7.0.

The CSE2 protein contains two possible bipartite nuclear localization signals and a putative basic-region leucine zipper (bZIP) (Fig. 4 and 5) (16, 61). Leucine zipper proteins usually contain at least four heptad repeats with leucine residues positioned on one face of the α-helix (32). A region of basic amino acids adjacent to the zipper permits bZIP proteins to bind to DNA, while the leucine zipper segment forms an α-helix that is implicated in protein dimerization (6, 25, 32, 45, 60, 61).

Although the CSE2 protein clearly resembles other bZIP proteins, the putative DNA-binding domain in CSE2 contains fewer basic amino acids than those of other bZIP proteins, and the spacer region lacks alanine residues (Fig. 5). CSE2 also contains a proline located between the heptad repeats and the basic region (Fig. 5). It has been proposed that proline residues introduce a kink into the α-helix, perhaps making it easier for long helical structures to wrap around globular proteins (3, 62). Computer-generated secondary structures for CSE2 predict that the heptad repeats form an α-helix and that the proline at position 119 is located in a predicted turn. Leucine zippers containing prolines have been proposed for several proteins, some of which are known to form dimers (for a review, see reference 6). Interestingly, a proline residue is present at an equivalent position in the bZIP structures proposed for CSE2 and a component of rat liver nucleosomes, macroH2A (Fig. 5) (42).

***CSE1* is essential for viability.** *CSE1* was disrupted by replacing 164 bp of the coding region with *LEU2* (Fig. 2A and Materials and Methods). The resulting heterozygote, M1702 (*cse1::LEU2/CSE1*), was sporulated, and four-spored asci were dissected. Each of the 48 tetrads examined produced only two viable spores, all of which were Leu$^-$. The presence of the *CSE1* allele in the Leu$^-$ segregants was confirmed by Southern hybridization (data not shown). Microscopy revealed that most (82%) of the presumed Leu$^+$ progeny stopped growing at the two-cell stage, indicating that the *CSE1* gene product is essential for vegetative growth but is not required for germination. The single-copy plasmid containing *CSE1*, p314P3.5, was shown to rescue the lethality caused by disruption of *CSE1* (data not shown).

Disruption of *CSE2* causes chromosome missegregation, slow growth, and conditional lethality. We disrupted the *CSE2* gene by inserting *LEU2* into the *Bam*HI site (p2020 [Fig. 2B and Materials and Methods]). Tetrad analysis of meiotic progeny from the resulting heterozygous disrupted strain (M2055) showed that *cse2::LEU2* haploid cells were viable, indicating that *CSE2* is not required for vegetative growth at 30°C. Haploid cells with the amino terminus of the CSE2 coding region removed were also viable (data not shown). Haploid *cse2::LEU2* strains exhibited a longer doubling time (133 min) than the wild type (100 min) and were both cold sensitive (15°C) and temperature sensitive (38°C). Homozygous *cse2::LEU2/cse2::LEU2* cells also grew significantly more slowly (doubling time, 120 min) than wild-type cells (90 min); however, no growth defect was observed for heterozygous cells (*cse2::LEU2/CSE2*) (94 min).

Our results suggest that the *cse2-1* and *cse2::LEU2* alleles have similar effects on the fidelity of chromosome segregation. The *X69* chromosome exhibited more segregation errors in *cse2::LEU2/cse2::LEU2* cells (12-fold more than the wild type) than in *cse2-1/cse2-1* cells (8-fold more than the wild type) (Table 2), partly because more loss events occurred in cells with the disrupted allele. Missegregation events involving chromosomes V and III (containing wild-

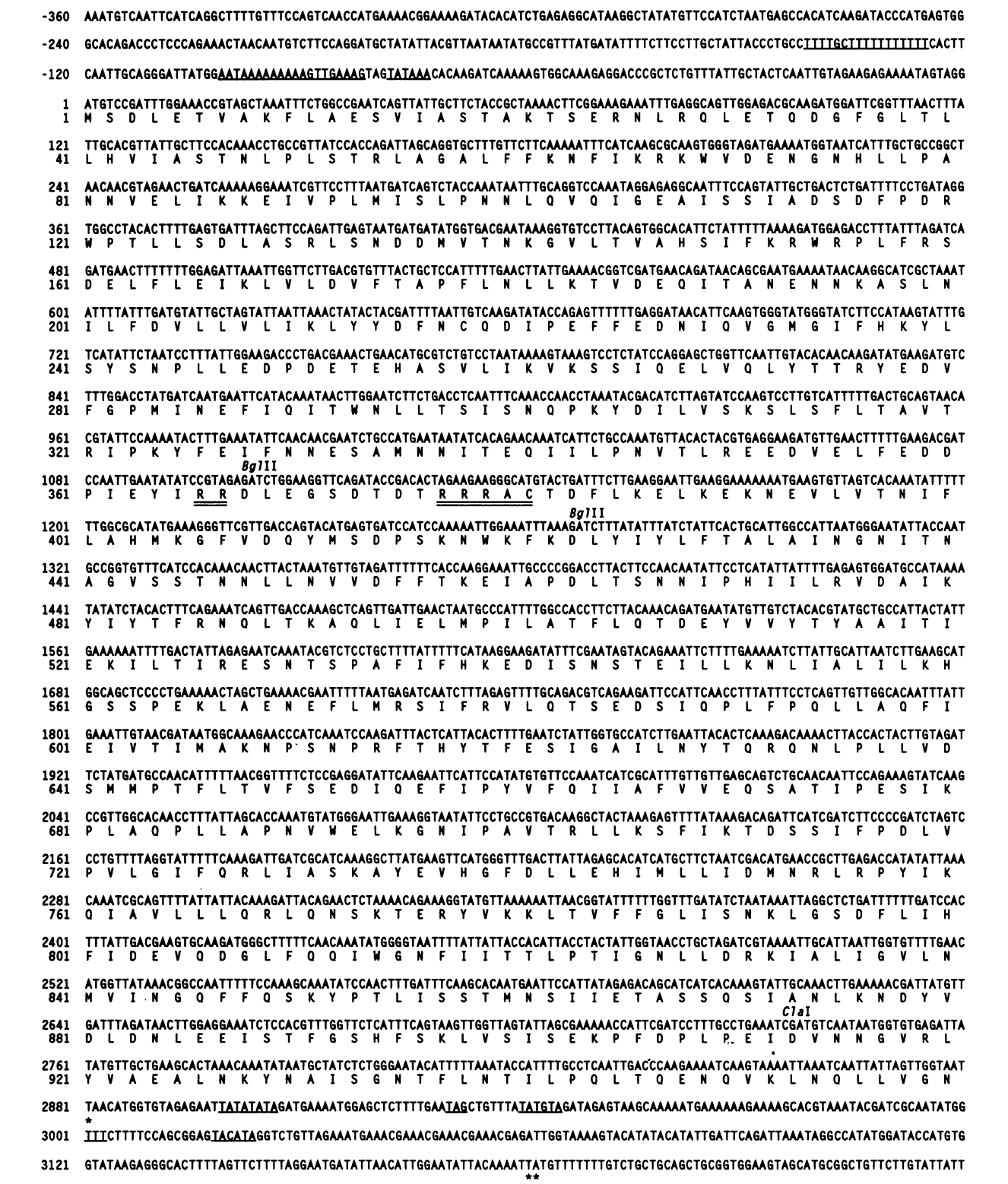

FIG. 3. Sequences of the *CSE1* gene and predicted protein. The nucleotide and amino acid residues are numbered on the left. The putative bipartite nuclear localization signal is indicated by the double underlines. The locations of potential promoter sequences, including TATA elements and an upstream poly(dA-dT) segment that could function as a constitutive promoter element, are denoted with single underlines (58). * denotes the CSE1 translation stop codon, and ** shows the position of the HAP2 stop codon. Potential polyadenylation and transcription termination signals (29, 47) are underlined in the 3′ noncoding region. Selected restriction sites are shown above the DNA sequence.

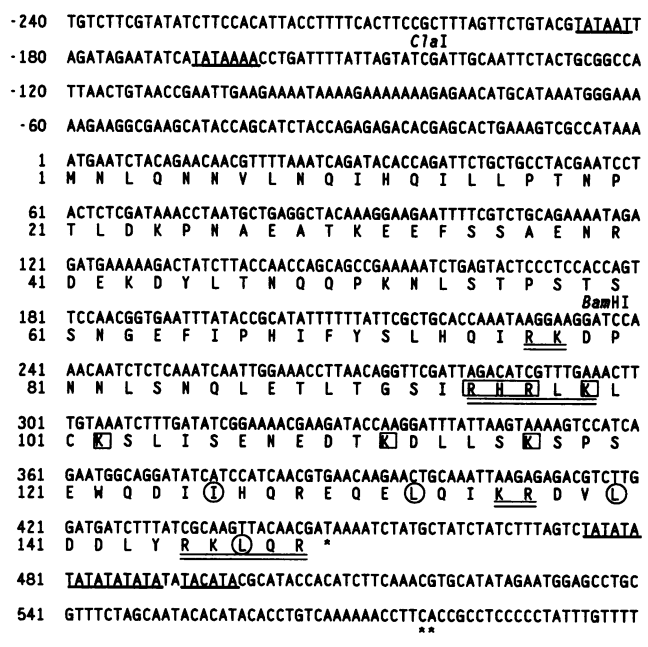

FIG. 4. Sequences of the *CSE2* gene and predicted protein. The nucleotide and amino acid residues are numbered on the left. The putative bipartite nuclear localization signals are indicated with double underlines. Hydrophobic amino acids in the putative leucine zipper are circled, and basic residues in the bZIP motif are boxed. * denotes the CSE2 translation stop codon, and ** indicates the PRP2 translation stop codon. The locations of potential TATA elements are underlined. Potential polyadenylation and transcription termination signals (29, 47) are underlined in the 3′ noncoding region.

type centromeres) increased 3-fold in *cse2-1/cse2-1* strains (Table 3), and 3- and 13-fold, respectively, in *cse2::LEU2/cse2::LEU2* strains. No increase in mitotic recombination was detected in *cse2::LEU2/cse2::LEU2* strains (data not shown).

***cse* arrest morphologies.** The cellular morphologies of *cse1-1*, *cse2-1*, and *cse2::LEU2* cells were examined at the nonpermissive temperature (11°C) (Fig. 6). After 48 h at 11°C, 46 to 58% of the *cse1-1*, *cse2-1*, and *cse2::LEU2* cells had arrested with large buds, compared with only 29% of the wild-type cells. A small fraction (4 to 6%) of the *cse* cells exhibited aberrant morphologies characterized by multiple, elongated buds. In addition, *cse1-1* cells often appeared swollen and enlarged.

The positions and morphologies of nuclei in the large-budded cells were analyzed by DAPI staining at the nonpermissive temperature (11°C) (Fig. 6). In the wild-type culture, 66% of the large-budded cells contained a nucleus in each of the mother and daughter cells (class III), compared with only 25, 19, and 41% of the *cse1-1*, *cse2-1*, and *cse2::LEU2* cells, respectively. Thirty-seven percent of the large-budded *cse2::LEU2* cells had single nuclei at or through the neck (class II), compared with 22 to 25% of the cells in the other cultures. Over 30% of the large-budded *cse1-1* and *cse2-1* cells had a single nucleus in the mother (class I), compared with 18% of the *cse2::LEU2* cells and 10% of the wild-type cells. Most notably, many of the *cse1-1* and *cse2-1* large-budded cells contained two nuclei in one cell body (20 and 25%, respectively [class IV]). The large-budded wild-type and *cse2::LEU2* cells did not contain a significant fraction of binucleate cells, possibly because a defective protein is made in *cse2-1* cells but is absent from cells carrying the *cse2::LEU2* null allele. Results similar to those shown in Fig. 6 were obtained for cells arrested for 24 h at 11°C (data not shown).

DISCUSSION

In this paper, we describe the characterization of two new genes isolated by using a genetic screen to detect chromosome segregation mutations. A chromosome containing a partially functional centromere was used in this study for two reasons. First, use of a chromosome with a segregation defect makes the screen sensitive enough to find mutations which might otherwise not be detected because of their mild effect on the transmission of chromosomes with wild-type centromeres. Second, since interactions between a mutant protein and the mutant centromere could result in a synthetic phenotype (26), this screen might yield genes encoding centromere-binding proteins. Mutations affecting the function of a kinetochore complex might dramatically affect the function of mutant centromeres but have little effect on wild-type centromeres.

Several lines of evidence indicate that the *CSE1* and *CSE2* gene products have a microtubule-related function in chromosome segregation and that they could play a direct role in centromere and kinetochore function. First, the *cse1-1* and *cse2-1* mutations have allele-specific effects on centromere function. For example, the *cse1-1* mutation causes a 10- to 14-fold increase in the missegregation of chromosomes with wild-type centromeres but increases missegregation of the *X78* chromosome 108-fold. Similarly, the *cse2-1* mutation increases missegregation of chromosomes with wild-type centromeres about 3-fold while increasing nondisjunction and loss of the *X35* chromosome 14-fold. Taken together, these data suggest a synthetic phenotype resulting from interactions between the *cse* mutant proteins and the mutant centromeres. Second, the *cse1-1* and *cse2-1* mutations cause primarily nondisjunction, not chromosome loss, and neither affects mitotic recombination. Third, the *cse1-1* and *cse2-1* mutants arrest predominantly as large-budded cells with the accumulation of binucleated cells (class IV [Fig. 6]) or a single nucleus (class I [Fig. 6]) in each mother cell, an indication that the *cse1-1* and *cse2-1* mutations may affect a microtubule-related function. Similar phenotypes have been observed for several previously described chromosome segregation mutants (20, 24, 53). In *S. cerevisiae*, microtubules are required for spindle pole body separation, spindle formation, chromosome separation, nuclear migration, and karyogamy (4, 27, 30, 46, 49). Support for the role of the *CSE1* and *CSE2* gene products in microtubule function comes from the fact that the *cse1-1* and *cse2-1* strains are more sensitive to the microtubule-depolymerizing drug nocodazole than wild-type cells but less sensitive than *tub* or *cin* mutants (24, 49). In addition, preliminary tubulin staining of arrested *cse* cells revealed that while many cells had microtubule structures appropriate for their stage of the cell cycle, some cells appeared to have deformed or abnormal spindle structures.

The *CSE1* gene is essential for cell growth. *CSE2* is not essential for cell viability, but an important function for the CSE2 protein is likely since disruption of the gene causes slow growth and aberrant chromosome segregation. Although both *cse* mutants have segregation defects, haploid *cse1-1 cse2-1* double mutants are viable and do not exhibit a synthetic lethal phenotype. Overexpression of *CSE2* does not rescue the cold sensitivity of *cse1-1* cells. However, one

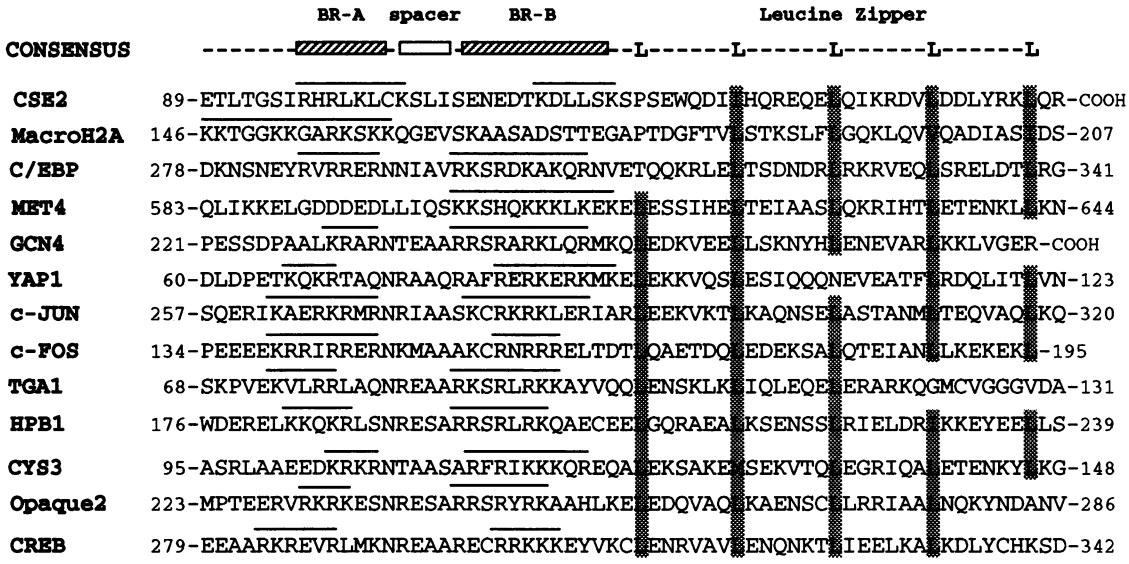

FIG. 5. Comparison of CSE2 and known bZIP proteins. The putative bZIP regions of 12 proteins are shown aligned with CSE2. The numbers preceding each sequence correspond to the position of the first amino acid shown in the indicated protein. The clusters of basic amino acids in each protein are indicated by a bar over the sequence, and the hydrophobic amino acids in the leucine zipper are shaded. The organization of the bZIP consensus elements is shown at the top (61). BR-A, basic region A; BR-B, basic region B. Protein sequences were taken from various references as follows: GCN4, YAP1, c-Jun, c-Fos, CREB, and C/EBP, reference 6; Opaque 2, TGA1, and HPB1, reference 59; macroH2A, reference 42; and CYS3, reference 17.

high-copy-number suppressor gene which rescues the cold-sensitive phenotype and partially suppresses the chromosome segregation defect of *cse1-1* cells has been cloned (10). This suppressor gene is identical to *SRP1* (63) and to a gene isolated independently in a screen for mutants displaying synthetic lethality with *bik1* (43). *SRP1-1* is an allele-specific dominant suppressor of temperature-sensitive mutations in the zinc-binding domain of yeast RNA polymerase I. The SRP1 protein is found associated with the nuclear envelope and could function in maintaining the structure of the nucleolus. Depletion of the SRP1 protein causes the accumulation of binucleated mother cells with anucleate daughter cells. *BIK1* encodes a microtubule-associated protein that colocalizes with tubulin in spindle pole bodies and the mitotic spindle (4). Therefore, both *BIK1* and *SRP1* have been implicated in microtubule-related functions. Taken together, these data are consistent with the notion that the *CSE1* gene product has a microtubule-related function in segregation. Alternatively, the *CSE* gene products could indirectly affect centromere function, perhaps by affecting the synthesis or processing of components required for spindle function or by altering a checkpoint required for proper chromosome segregation (22). It has been shown that plasmids with mutant centromeres induce a mitotic delay, suggesting that one checkpoint monitors the attachment of the chromosomes to the spindle (55). Presumably, mutations in genes required for this checking function would enhance the deleterious effects of centromere mutations.

The observation that the *cse1-1* and *cse2-1* mutations affect the function of the CDEII mutants suggests that the CSE proteins could interact with CDEII. So far, no CDEII binding protein(s) has been identified. However, data from DNase I protection experiments with either isolated nuclei (48) or the CDEIII-binding protein complex, CBF3 (33), as well as in vivo footprinting studies (15), indicate that the DNA at the junction of CDEII and CDEIII is protected by

A

	UB	SB	LB	AM
WT	43	27	29	<1
cse1-1	28	9	58	4
cse2-1	27	20	46	6
cse2::LEU2	30	13	49	6

B

Class	I	II	III	IV
WT	10	22	66	<1
cse1-1	33	22	25	20
cse2-1	31	25	19	25
cse2::LEU2	18	37	41	3

FIG. 6. Cell morphologies at the restrictive temperature in *cse* strains. Wild-type (WT; *CSE*$^+$) and *cse* strains were analyzed after 48 h at 11°C. Similar results were obtained for the 24-h time point. (A) Percentages of cells with the indicated morphology: UB, unbudded; SB, small budded; LB, large budded; and AM, abnormal morphology such as multibudded or very elongated cell bodies. (B) Percentages of large-budded cells with the nuclear DNA staining region indicated in class I to class IV. Strains: Y1706 (*CSE*$^+$), Y1705 (*cse1-1*), Y2009 (*cse2-1*), and M2056 (*cse2::LEU2*).

protein. How the centromere DNA, centromere-binding proteins, and probably histones associate to form the structure of the yeast kinetochore is not known.

The CSE2 protein contains a potential bZIP motif which is used for DNA binding by many transcription factors. However, we do not know whether the CSE2 protein can bind DNA, and if so, whether the CSE2 protein could mediate interactions between the chromosome and the microtubule or microtubule-associated proteins. Alternatively, the CSE2 protein could be a transcription factor that regulates expression of components required for mitosis. The latter model predicts that the CSE2 protein is required for the expression of genes whose products are critical for centromere function. These possibilities are currently under investigation.

ACKNOWLEDGMENTS

We thank T. Mason for many useful suggestions, P. Hieter for the pRS vectors, T. Stearns for the *tub* and *cin* strains, and J. King for the meiotic mapping program. We are grateful to B. Byers for allowing some of this work to be completed in his laboratory. We thank A. Gaudet for many helpful and stimulating discussions and critical reading of the manuscript and K. Curnick and L. Densmore for data base management. We thank our colleagues in the laboratory of M.F.-H. for suggestions and comments throughout this study.

This work was supported by a U.S. Public Health Service grant (GM32257) and a Research Career Development Award (GM00528) from the National Institutes of Health to M.F.-H.

REFERENCES

1. **Baker, R. E., M. Fitzgerald-Hayes, and T. C. O'Brien.** 1989. Purification of the yeast centromere binding protein CP1 and a mutational analysis of its binding site. J. Biol. Chem. **264:**10843–10850.
2. **Baker, R. E., and D. C. Masison.** 1990. Isolation of the gene encoding the *Saccharomyces cerevisiae* centromere-binding protein CP1. Mol. Cell. Biol. **10:**2458–2467.
3. **Barlow, D. J., and J. M. Thornton.** 1988. Helix geometry in proteins. J. Mol. Biol. **201:**601–619.
4. **Berlin, V., C. A. Styles, and G. R. Fink.** 1990. BIK1, a protein required for microtubule function during mating and mitosis in *Saccharomyces cerevisiae*, colocalizes with tubulin. J. Cell Biol. **111:**2573–2586.
5. **Boeke, J. D., F. LaCroute, and G. R. Fink.** 1984. A positive selection for mutants lacking orotidine-5′-phosphate decarboxylase activity in yeast: 5-fluoro-orotic acid resistance. Mol. Gen. Genet. **197:**345–346.
6. **Busch, S. J., and P. Sassone-Corsi.** 1990. Dimers, leucine zippers and DNA-binding domains. Trends Genet. **6:**36–40.
7. **Cai, M., and R. W. Davis.** 1989. Purification of a yeast centromere-binding protein that is able to distinguish single base-pair mutations in its recognition site. Mol. Cell. Biol. **9:**2544–2550.
8. **Cai, M., and R. W. Davis.** 1990. Yeast centromere binding protein CBF1, of the helix-loop-helix protein family, is required for chromosome stability and methionine prototrophy. Cell **61:**437–446.
9. **Chen, J.-H., and R.-J. Lin.** 1990. The yeast PRP2 protein, a putative RNA-dependent ATPase, shares extensive sequence homology with two other pre-mRNA splicing factors. Nucleic Acids Res. **18:**6447.
10. **Chen, X. H., Z. Xiao, and M. Fitzgerald-Hayes.** Unpublished data.
11. **Chu, G., D. Vollrath, and R. W. Davis.** 1986. Separation of large DNA molecules by contour-clamped homogeneous electric fields. Science **234:**1582–1585.
12. **Clarke, L., and J. Carbon.** 1983. Genomic substitutions of centromeres in *Saccharomyces cerevisiae*. Nature (London) **305:**23–28.
13. **Cottarel, G., J. H. Shero, P. Hieter, and J. H. Hegemann.** 1989. A 125-base-pair *CEN6* DNA fragment is sufficient for complete meiotic and mitotic centromere functions in *Saccharomyces cerevisiae*. Mol. Cell. Biol. **9:**3342–3349.
14. **Cumberledge, S., and J. Carbon.** 1987. Mutational analysis of meiotic and mitotic centromere function in *Saccharomyces cerevisiae*. Genetics **117:**203–212.
15. **Densmore, L., W. E. Payne, and M. Fitzgerald-Hayes.** 1991. In vivo genomic footprint of a yeast centromere. Mol. Cell. Biol. **11:**154–165.
16. **Dingwall, C., and R. A. Laskey.** 1991. Nuclear targeting sequences—a consensus? Trends Biochem. Sci. **16:**478–481.
17. **Fu, Y.-H., J. V. Paietta, D. G. Mannix, and G. A. Marzluf.** 1989. *cys-3*, the positive-acting sulfur regulatory gene of *Neurospora crassa*, encodes a protein with a putative leucine zipper DNA-binding element. Mol. Cell. Biol. **9:**1120–1127.
18. **Gaudet, A., and M. Fitzgerald-Hayes.** 1987. Alterations in the adenine-plus-thymine-rich region of *CEN3* affect centromere function in *Saccharomyces cerevisiae*. Mol. Cell. Biol. **7:**68–75.
19. **Gaudet, A., and M. Fitzgerald-Hayes.** 1989. Mutations in *CEN3* cause aberrant chromosome segregation during meiosis in *Saccharomyces cerevisiae*. Genetics **121:**447–489.
20. **Gerring, S. L., F. Spencer, and P. Hieter.** 1990. The *CHL* (*CTF1*) gene product of *Saccharomyces cerevisiae* is important for chromosome transmission and normal cell cycle progression in G2/M. EMBO J. **9:**4347–4358.
21. **Hartwell, L. H., and D. Smith.** 1985. Altered fidelity of mitotic chromosome transmission in cell cycle mutants of *S. cerevisiae*. Genetics **110:**381–395.
22. **Hartwell, L. H., and T. A. Weinert.** 1989. Checkpoints: controls that ensure the order of cell cycle events. Science **246:**629–634.
23. **Hieter, P., C. Mann, M. Snyder, and R. W. Davis.** 1985. Mitotic stability of yeast chromosomes: a colony color assay that measures nondisjunction and chromosome loss. Cell **40:**381–392.
24. **Hoyt, M. A., T. Stearns, and D. Botstein.** 1990. Chromosome instability mutants of *Saccharomyces cerevisiae* that are defective in microtubule-mediated processes. Mol. Cell. Biol. **10:**223–234.
25. **Hu, J. C., E. K. O'Shea, P. S. Kim, and R. T. Sauer.** 1990. Sequence requirements for coiled-coils: analysis with lambda repressor-GCN4 leucine zipper fusion. Science **250:**1400–1403.
26. **Huffaker, T. C., M. A. Hoyt, and D. Botstein.** 1987. Genetic analysis of the yeast cytoskeleton. Annu. Rev. Genet. **21:**259–284.
27. **Huffaker, T. C., J. H. Thomas, and D. Botstein.** 1988. Diverse effects of β-tubulin mutations on microtubule formation and function. J. Cell Biol. **106:**1997–2010.
28. **Hyman, A. A., K. Middleton, M. Centola, T. J. Mitchison, and J. Carbon.** 1992. Microtubule-motor activity of a yeast centromere-binding protein complex. Nature (London) **359:**533–536.
29. **Irniger, S., C. M. Egli, and G. H. Braus.** 1991. Different classes of polyadenylation sites in the yeast *Saccharomyces cerevisiae*. Mol. Cell. Biol. **11:**3060–3069.
30. **Jacobs, C. W., A. E. M. Adams, P. J. Szaniszlo, and J. R. Pringle.** 1988. Functions of microtubules in the *Saccharomyces cerevisiae* cell cycle. J. Cell Biol. **107:**1409–1426.
31. **Jiang, W., and P. Philippsen.** 1989. Purification of a protein binding to the CDEI subregion of *Saccharomyces cerevisiae* centromere DNA. Mol. Cell. Biol. **9:**5585–5593.
32. **Landschulz, W. H., P. F. Johnson, and S. L. McKnight.** 1988. The leucine zipper: a hypothetical structure common to a new class of DNA binding proteins. Science **240:**1759–1764.
33. **Lechner, J., and J. Carbon.** 1991. A 240 kb multisubunit protein complex, CBF3, is a major component of the budding yeast centromere. Cell **64:**717–725.
34. **McGrew, J., B. Diehl, and M. Fitzgerald-Hayes.** 1986. Single base-pair mutations in centromere element III cause aberrant chromosome segregation in *Saccharomyces cerevisiae*. Mol. Cell. Biol. **6:**530–538.
35. **McGrew, J. T., Z. Xiao, and M. Fitzgerald-Hayes.** 1989. *Saccharomyces cerevisiae* mutants defective in chromosome segregation. Yeast **5:**271–284.
36. **Mellor, J., J. Rathjen, W. Jiang, and S. J. Dowell.** 1991. DNA binding of CPF1 is required for optimal centromere function but not for maintaining methionine protrophy in yeast. Nucleic

Acids Res. **19**:2961–2969.
37. **Mortimer, R. K., R. Contopoulou, and D. Schild.** 1981. Mitotic chromosome loss in a radiation-sensitive strain of the yeast *Saccharomyces cerevisiae*. Proc. Natl. Acad. Sci. USA **78**: 5778–5782.
38. **Mortimer, R. K., and D. Schild.** 1980. Genetic map of *Saccharomyces cerevisiae*. Microbiol. Rev. **44**:519–571.
39. **Murphy, M. R., D. M. Fowlkes, and M. Fitzgerald-Hayes.** 1991. Analysis of centromere function in *Saccharomyces cerevisiae* using synthetic centromere mutants. Chromosoma **101**:189–197.
40. **Ng, R., and J. Carbon.** 1987. Mutational and in vitro protein-binding studies on centromere DNA from *Saccharomyces cerevisiae*. Mol. Cell. Biol. **7**:4522–4534.
41. **Palmer, R. E., E. Hogan, and D. Koshland.** 1990. Mitotic transmission of artificial chromosomes in *cdc* mutants of the yeast, *Saccharomyces cerevisiae*. Genetics **125**:763–774.
42. **Pehrson, J. R., and V. A. Fried.** 1992. MacroH2A, a core histone containing a large nonhistone region. Science **257**:1398–1400.
43. **Pellman, D.** 1993. Personal communication.
44. **Pinkham, J. L., J. T. Olesen, and L. P. Guarente.** 1987. Sequence and nuclear localization of the *Saccharomyces cerevisiae* HAP2 protein, a transcriptional activator. Mol. Cell. Biol. **7**:578–585.
45. **Ransone, L. J., J. Visvader, P. Sassone-Corsi, and I. M. Verma.** 1989. Fos-Jun interaction: mutational analysis of the leucine zipper domain of both proteins. Genes Dev. **3**:770–781.
46. **Rose, M. D., and G. R. Fink.** 1987. *KAR1*, a gene required for function of both intranuclear and extranuclear microtubules in yeast. Cell **48**:1047–1060.
47. **Russo, P., W.-Z. Li, D. M. Hampsey, K. S. Zaret, and F. Sherman.** 1991. Distinct *cis*-acting signals enhance 3′ endpoint formation of *CYC1* mRNA in the yeast *Saccharomyces cerevisiae*. EMBO J. **10**:563–571.
48. **Saunders, M., M. Fitzgerald-Hayes, and K. Bloom.** 1988. Chromatin structure of altered yeast centromeres. Proc. Natl. Acad. Sci. USA **85**:175–179.
49. **Schatz, P. J., F. Solomon, and D. Botstein.** 1988. Isolation and characterization of conditional-lethal mutations in the *TUB1* α-tubulin gene of the yeast *Saccharomyces cerevisiae*. Genetics **120**:681–695.
50. **Sharp, P. M., and E. Cowe.** 1991. Synonymous codon usage in *Saccharomyces cerevisiae*. Yeast **7**:657–678.
51. **Sherman, F., G. R. Fink, and J. B. Hicks.** 1986. Laboratory course manual for methods in yeast genetics. Cold Spring Harbor Laboratory, Cold Spring Harbor, N.Y.
52. **Sikorski, R. S., and P. Hieter.** 1989. A system of shuttle vectors and yeast host strains designed for efficient manipulation of DNA in *Saccharomyces cerevisiae*. Genetics **122**:19–27.
53. **Snyder, M., and R. W. Davis.** 1988. *SPA1*: a gene important for chromosome segregation and other mitotic functions in *S. cerevisiae*. Cell **54**:743–754.
54. **Sokal, R. R., and F. J. Rohlf.** 1981. Biometry. W. H. Freeman & Co., San Francisco.
55. **Spencer, F., and P. Hieter.** 1992. Centromere DNA mutations induce a mitotic delay in *Saccharomyces cerevisiae*. Proc. Natl. Acad. Sci. USA **89**:8908–8912.
56. **Spencer, J., S. L. Gerring, C. Connelly, and P. A. Hieter.** 1990. Mitotic chromosome transmission fidelity mutants in *Saccharomyces cerevisiae*. Genetics **124**:237–249.
57. **Stearns, T., M. A. Hoyt, and D. Botstein.** 1990. Yeast mutants sensitive to antimicrotubule drugs define three genes that affect microtubule function. Genetics **124**:251–262.
58. **Struhl, K.** 1985. Naturally occurring poly(dA-dT) sequences are upstream promoter elements for constitutive transcription in yeast. Proc. Natl. Acad. Sci. USA **82**:8419–8423.
59. **Thomas, D., I. Jacquemin, and Y. Surdin-Kerjan.** 1992. MET4, a leucine zipper protein, and centromere-binding factor 1 are both required for transcriptional activation of sulfur metabolism in *Saccharomyces cerevisiae*. Mol. Cell. Biol. **12**:1719–1727.
60. **Turner, R., and R. Tjian.** 1989. Leucine repeats and an adjacent DNA binding domain mediate the formation of functional cFos-cJun heterodimers. Science **243**:1689–1694.
61. **Vinson, C. R., P. B. Sigler, and S. L. McKnight.** 1989. Scissors-grip model for DNA recognition by a family of leucine zipper proteins. Science **246**:911–916.
62. **Woolfson, D. N., and D. H. Williams.** 1990. The influence of proline residues on α-helical structure. FEBS Lett. **277**:185–188.
63. **Yano, R., M. Oakes, M. Yamaghishi, J. A. Dodd, and M. Nomura.** 1992. Cloning and characterization of *SRP1*, a suppressor of temperature-sensitive RNA polymerase I mutations, in *Saccharomyces cerevisiae*. Mol. Cell. Biol. **12**:5640–5651.